JCI insight

RESEARCH ARTICLE

# Exosomal Tat protein activates latent HIV-1 in primary, resting CD4+ T lymphocytes

**Xiaoli Tang,[1] Huafei Lu,[1] Mark Dooner,[2] Stacey Chapman,[3] Peter J. Quesenberry,[2] and Bharat Ramratnam[1, 4, 5]**

[1]Division of Infectious Diseases and [2]Division of Hematology and Oncology, Department of Medicine, Rhode Island Hospital and Warren Alpert Medical School of Brown University, Providence, Rhode Island, USA. [3]Center for AIDS Research, The Miriam Hospital, Providence, Rhode Island, USA. [4]Lifespan Clinical Research Center, Providence, Rhode Island, USA. [5]COBRE Center for Cancer Research Development, Rhode Island Hospital, Providence, Rhode Island, USA.

**Replication competent HIV-1 persists in a subpopulation of CD4+ T lymphocytes despite prolonged antiretroviral treatment. This residual reservoir of infected cells harbors transcriptionally silent provirus capable of reigniting productive infection upon discontinuation of antiretroviral therapy. Certain classes of drugs can activate latent virus but not at levels that lead to reductions in HIV-1 reservoir size in vivo. Here, we show the utility of CD4+ receptor targeting exosomes as an HIV-1 latency reversal agent (LRA). We engineered human cellular exosomes to express HIV-1 Tat, a protein that is a potent transactivator of viral transcription. Preparations of exosomal Tat-activated HIV-1 in primary, resting CD4+ T lymphocytes isolated from antiretroviral-treated individuals with prolonged periods of viral suppression and led to the production of replication competent HIV-1. Furthermore, exosomal Tat increased the potency of selected LRA by over 30-fold in terms of HIV-1 mRNA expression, thereby establishing it as a potentially new class of biologic product with possible combinatorial utility in targeting latent HIV-1.**

## Introduction

Highly active antiretroviral treatment (HAART) of HIV-1 eliminates productively infected cells, with plasma levels of virus being reduced to levels below the limit of detection of current assays (1–3). While treatment leads to the reduction in total body viral burden, a relatively small but stable reservoir of latently infected cells remains (4–6). Not surprisingly, when HAART is stopped, activation of infected reservoir cells eventually leads to plasma viremia in most individuals (7, 8). Thus, a major roadblock to HIV-1 cure is the inability to eliminate latently infected cells despite prolonged antiretroviral therapy.

Transcriptional activation of latent HIV-1 has long served as a potential strategy to purge viral reservoirs with the hope that productively infected cells will succumb to viral cytopathicity or immune clearance under the cover of antiretroviral therapy (9, 10). Early attempts used biologics such as OKT3 but were accompanied by adverse effects such as global immune stimulation and prolonged periods of CD4+ T lymphocyte depletion (11). Recent efforts have centered on the identification of latency reversal agents (LRA) that activate virus without immune stimulation (3, 6, 7, 12, 13). Two Food and Drug Administration–approved (FDA-approved) drugs (histone deacetylase [HDAC] inhibitors and disulfiram [Dis]) appear to reverse HIV-1 latency in vitro, but clinical studies have not demonstrated significant reduction in the size of the latent reservoir in the limited number of individuals studied (12–14).

Interestingly, the Tat protein encoded by HIV-1 itself is perhaps one of the most potent enhancers of viral transcription. This protein activates the HIV-1 promoter present in the long terminal repeat (LTR) region of proviruses that have undergone transcriptional activation. While the presence of Tat appears sufficient to reverse HIV-1 latency, mechanisms to practically harness this protein as an LRA have not been extensively explored (15–17). A prime challenge of protein therapeutics is their cost-effective manufacture and targeted cellular delivery. We reasoned that recent advances in exosome biology would allow us to package HIV-1 Tat in extracellular vesicles for targeted delivery to latently infected CD4+ T lymphocytes, leading to viral reactivation.

**Conflict of interest:** The authors have declared that no conflict of interest exists.

**Submitted:** June 13, 2017
**Accepted:** February 28, 2018
**Published:** April 5, 2018

**Reference information:**
*JCI Insight*. 2018;3(7):e95676. https://doi.org/10.1172/jci.insight.95676.

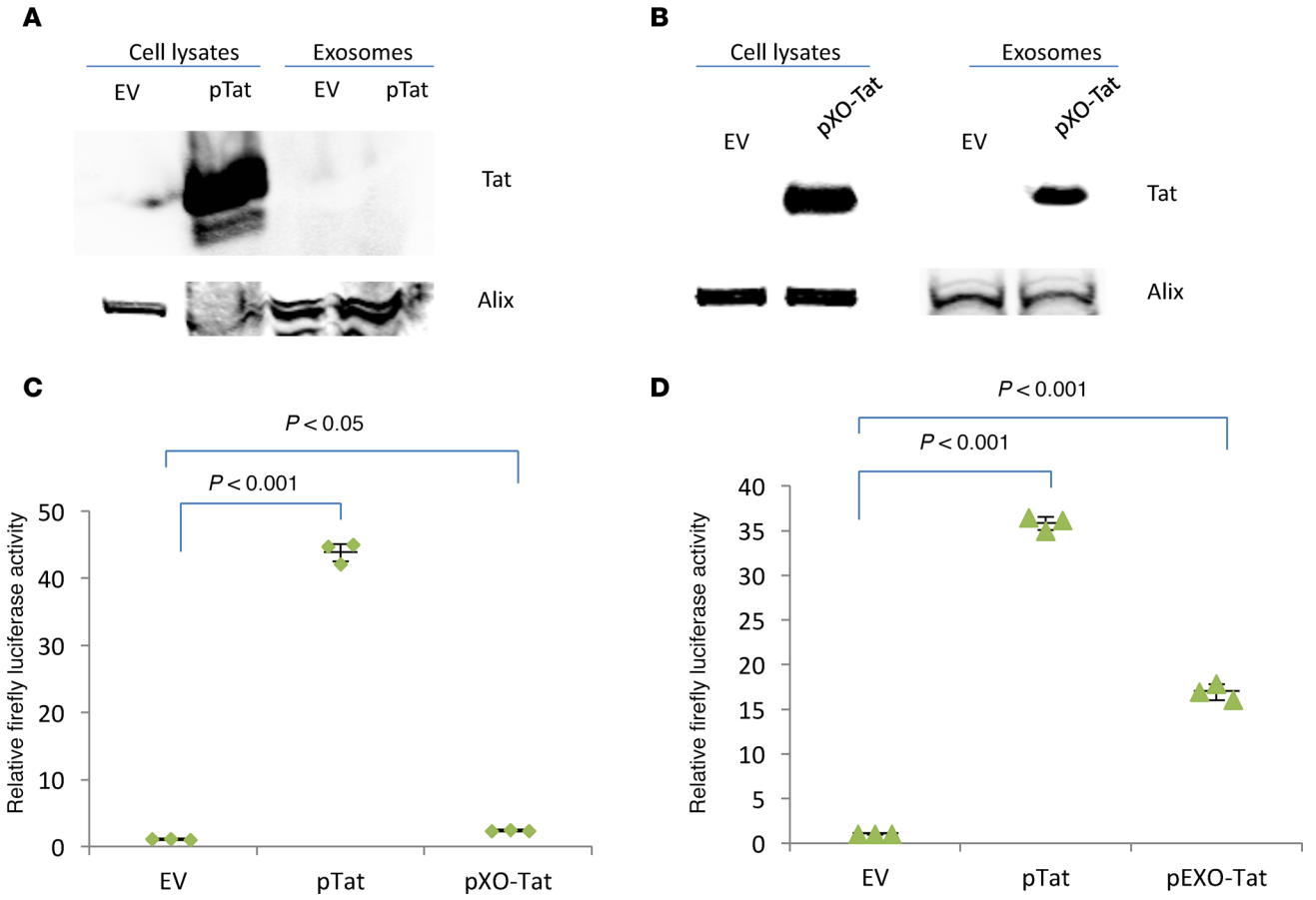


**Figure 1. Exosomal localization and biological activity of modified HIV-1 Tat expression vectors.** (**A**) Using an expression vector encoding WT HIV-1 Tat (pTat), we profiled protein levels in cell lysates of transfected HEK293T cells, as well as in released exosomes of 30–150 nm in diameter. Western blot revealed robust expression of Tat in cellular lysates but not in released exosomes. An empty expression vector (EV) was used as a control. The exosome marker Alix was used to control for protein loading. (**B**) We modified the Tat expression vector to include a peptide sequence that targets proteins to the interior exosomal membrane (pXO-Tat). Western blot of transfected HEK293T cells revealed Tat protein expression in both cellular lysates and exosomal preparations. No Tat protein was detected with use of the EV. The exosome marker Alix was used to control for protein loading. (**C** and **D**) The TZM-bl cell line was used to quantify the transactivating activity of Tat produced by WT (pTat), exosomal localization modified (pXO-Tat), and nuclear/exosomal localization modified (pEXO-Tat) EVs. Exosomal localization (pXO-Tat) decreased transactivating activity that depends upon nuclear localization of Tat (**C**). Inclusion of a c-Myc nuclear localization signal (NLS) increased activity to ~50% of WT Tat levels (pTat) (**D**). Experiments were performed in triplicate with 2 technical replicates. Quantitative data was analyzed by ANOVA with between-group comparisons evaluated with post-hoc Tukey-Kramer HSD tests, which correct for multiple comparison. Data are expressed as mean ± SEM. $P < 0.05$ indicates statistical significance.

## Results

*Engineering HIV-1 Tat expression in exosomes*. We began by asking whether HIV-1 *Tat* was present in extracellular vesicles released by cells that expressed the protein. As seen in Figure 1A, transfection of a Tat plasmid expression vector (denoted as pTat) into HEK293T cells led to robust levels of intracellular Tat but no detectable expression in released exosomes of 30–150 nm diameter. We modified our expression vector to include a previously characterized peptide sequence that, when placed upstream of the coding sequence, directs proteins to the interior exosomal membrane (18). The modified vector (pXO-Tat) was transfected into HEK293T cells and led to robust expression of Tat in released exosomes (Figure 1B). We next tested the function of our modified Tat construct in TZM-bl cells, an indicator cell line that enables quantitative analysis of HIV-1 promoter LTR activation using either luciferase or β-gal as a reporter (19). Transfection of pXO-Tat into TZM-bl cells significantly increased HIV-1 promoter LTR activation but at levels far less than that of WT pTat (Figure 1C). Given that the biological activity of Tat derives from its nuclear localization, we reasoned that our placement of a membrane localization signal allowed shuttling between plasma membrane and nuclear compartments, reducing Tat protein levels in the latter and, thereby, HIV-1 transactivating activity. To retain exosomal localization yet increase nuclear presence, we fused a c-Myc nuclear

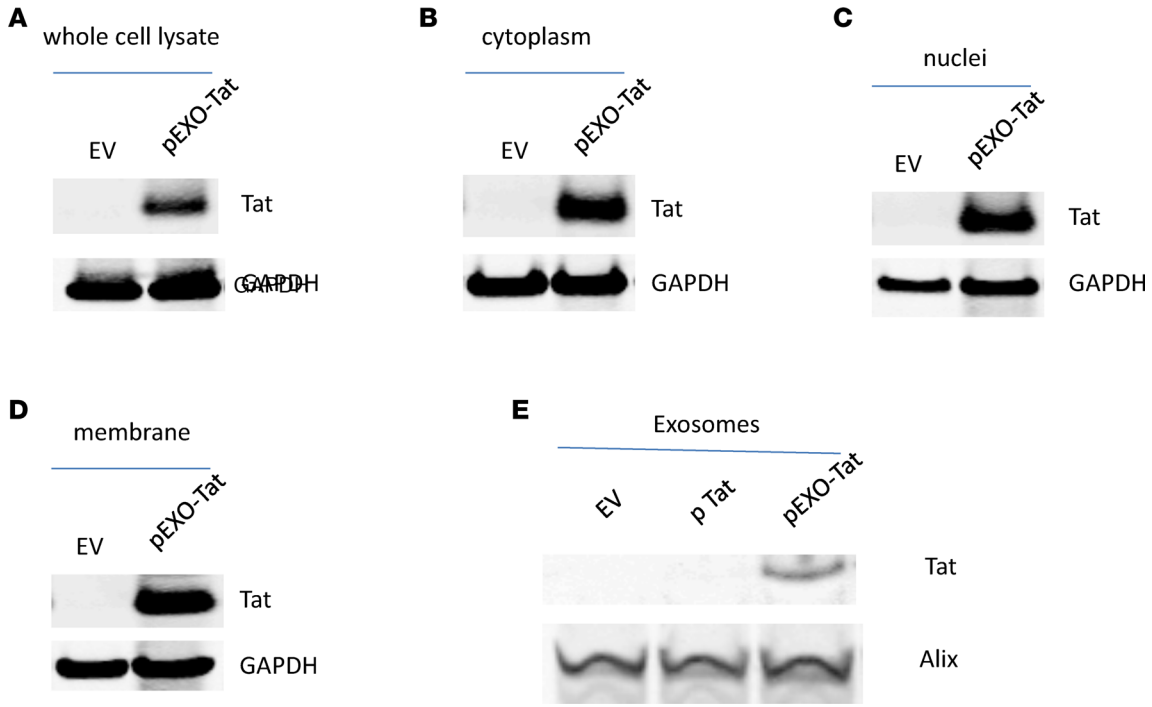


**Figure 2. Subcellular localization of engineered EXO-Tat protein.** HEK293T cells were maintained in culture and transfected by pEXO-Tat or an empty expression vector (EV). Cells and supernatants were fractionated, and Western blot revealed Tat expression in all cellular fractions examined, as well as in released exosomes. GAPDH was used to control for protein loading in experiments involving cellular fractions, and Alix was used for those involving exosomal preparations. No Tat protein was detected in parallel experiments involving the transfection of an EV. EXO-Tat protein expression in whole cell lysate (**A**), cytoplasmic fraction (**B**), nuclear fraction (**C**), membranous fraction (**D**), and released exosomes (**E**).

localization signal (NLS) to the C-terminus of Tat. The biological activity of this new plasmid expression vector (denoted as pEXO-Tat) was quantified using the TZM-bl reporter system with pEXO-Tat activating the HIV-1 promoter LTR 9-fold more than pXO-Tat with about 50% potency of WT pTat (Figure 1D). The subcellular distribution of EXO-Tat was profiled by Western blot. As seen in Figure 2, Tat protein could be readily detected not only in cytoplasmic, nuclear, and membrane fractions, but also in a heterogeneous population of released extracellular vesicles.

To further verify that our manipulation of the N- and C-terminal sequences of Tat had no impact on its transactivating activity, we used U1 cells, a promonocytic cell line engineered to harbor integrated HIV-1 (20). U1 cells have minimal levels of baseline viral expression that increase after treatment with agents that activate the HIV-1 LTR. Transfection of pEXO-Tat into U1 cells led to an increase in virion release, as quantified by serial p24 protein measurement in cellular supernatants (Figure 3A). These data were duplicated using other in vitro models of HIV-1 latency, including the J-Lat GFP (clone A72) in which viral promoter (LTR) activation is tracked by GFP expression (21). As seen in Figure 3B, transfection of pEXO-Tat into J-Lat GFP cells led to 3-fold increase in GFP protein expression compared with relevant controls, as quantified by Western blot. Thus, using a variety of different cellular models, we verified that modification of the Tat backbone with the inclusion of nuclear and membrane localization signals did not abrogate its ability to transcriptionally activate the viral LTR. We next focused our experiments on testing the activity of exosomes harboring Tat in primary resting $CD4^+$ T lymphocytes.

*Exosomal Tat activates latent HIV-1 in primary resting $CD4^+$ T lymphocytes.* Thus far, we had used transient transfection of our constructs to generate EXO-Tat exosomes. Typically, transient transfections led to robust exosome production over a period of 2–4 days, after which cell overgrowth and death ensued. To facilitate downstream experiments, we increased the scale of production by transduction of HEK293T cells with a lentiviral construct harboring our EXO-Tat expression system. Cells were placed under drug selection, and serial sampling of cell lysates revealed robust, continuous Tat production after 15 days of drug selection (Figure 4A). Given that all cells examined to date produce exosomes, we expect that our lentiviral transduction led to Tat protein expression in exosomes produced by HEK293 cells, but we are not

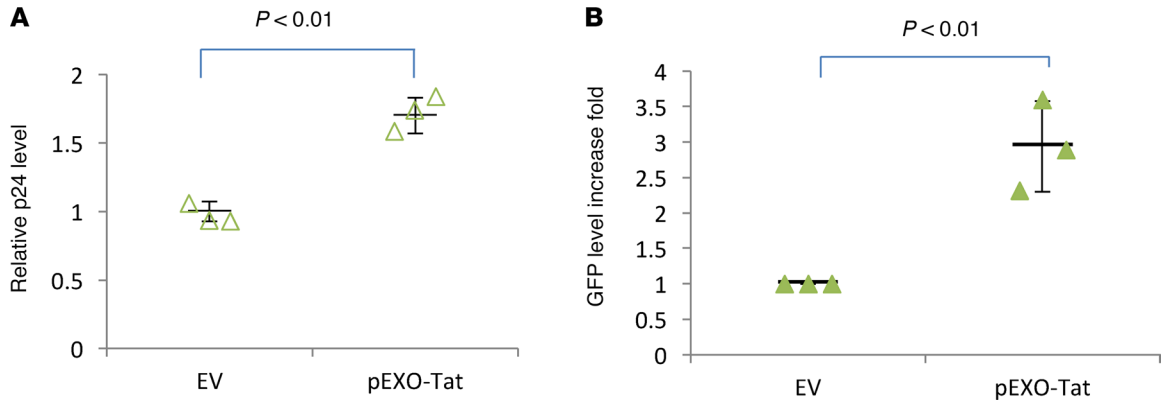


**Figure 3. EXO-Tat activates the HIV-1 LTR promoter in in vitro models of viral latency.** We used 2 well-characterized cellular models to quantify the effect of EXO-Tat on viral activity. (**A**) Transfection of pEXO-Tat into U1 cells that harbor integrated HIV-1 led to increased virion production and release as quantified by HIV-1 p24 antigen levels in culture supernatant over a 48-hour period. P24 levels were normalized to values obtained with control experiments involving the transfection of an empty expression vector (EV). (**B**) The J-Lat GFP (clone A72) cell line allows quantification of viral promoter (LTR) activation by GFP expression. Under fluorescent microscope, most of the untreated cells express GFP, albeit some GFP signals were very weak. By flow cytometry, we could detect 20.6% GFP-positive cells in untreated condition or 3 days after tranfection of an empty vector (EV). Transfection of pEXO-Tat increased GFP positive cells to 22.2%. In terms of total GFP protein level, transfection of pEXO-Tat into J-Lat GFP cells led to 3-fold increase in GFP expression compared with experiments involving the EV. Blot band intensity was measured using the Licor Odyssey software. Two-tailed unpaired Student's *t* test was performed; $P < 0.05$ indicates statistical significance. Experiments were performed in duplicate with 3 technical replicates.

able to quantify the fraction of exosomes harboring Tat. Technically, experimental means to visualize Tat or any protein on a single exosome basis are not available, given the virus-like size of the particles and the limited resolution of techniques such as flow cytometry. We next stained exosomes with a highly lipophilic dye (DIO) and used flow cytometry to quantify exosomal cellular uptake kinetics. As seen in Figure 4B, ~13% of $CD4^+$ T lymphocytes were $DiO^+$, in agreement with results obtained using immunofluorescent staining (Figure 4C).

We next used primary, resting [$HLA\text{-}DR^-$, $CD25^-$, $CD69^-$] $CD4^+$ T lymphocytes isolated from 7 HIV-1–infected individuals successfully treated with antiretroviral drugs with prolonged periods of viral suppression (patients #211, #219, #232, #111, #112, #204, and #207 in Table 1). We first tested the latency reversal potency of exosomes by treating resting $CD4^+$ T cells ($rCD4^+$ T cells) with increasing numbers of exosomes (0, $9 \times 10^8$, $1.8 \times 10^9$, $3.6 \times 10^9$). We found that maximal LTR activation occurred at a dose of $1.8 \times 10^9$ without any appreciable cell death and used this dose for all downstream experiments. Highly purified preparations of $rCD4^+$ cells (~$2 \times 10^6$) were placed in culture and treated with control exosomes (Exo-C) or exosomes harboring EXO-Tat ($1.8 \times 10^9$ exosomes or 46.8 μg total protein) for 96 hours. As seen in Figure 5, A and B, EXO-Tat exosomal treatment led to the expression of HIV-1 unspliced RNA in all 7 individuals. Levels of intracellular HIV-1 RNA were below the level of detection in $rCD4^+$ lymphocytes treated with Exo-C in every case examined. We next subjected cellular RNA to Tat/rev induced limiting dilution assay (TILDA) (22). This PCR reaction measures inducible multiply spliced HIV RNA (msRNA), the presence of which is thought to correlate with replication competent HIV-1. We found that 4 (patients #211, #219, #112, and #207) out of 5 patient samples were positive for tat/rev msRNA. In 3 cases, for which we had sufficient $rCD4^+$ cells for multiple replicate experiments (patients #204, #112, and #211), we compared the latency reversing potency of EXO-Tat exosomes with that of 2 LRAs, panobinostat (Pan) and Dis. As seen in Figure 5, C and D, cultures employed a variety of control and experimental conditions. Treatment of $rCD4^+$ cells only with 30 nM Pan or 500 nM Dis did not lead to an increase in intracellular HIV-1 RNA compared with relevant controls. Interestingly, addition of both EXO-Tat and LRA increased viral reactivation by 30-fold, as compared with experiments only using EXO-Tat.

While nucleic acid–based assays can quantify the transcription of integrated HIV-1, the mere presence of transcription does not always correlate with cellular production and release of infectious virions. In the majority of cells infected by HIV-1, integrated virus is defective due to the error-prone nature of the viral enzyme reverse transcriptase that converts incoming virion RNA into DNA. To confirm that EXO-Tat exosomes reactivated latent HIV-1 to produce replication-competent virus, we isolated $rCD4^+$ T cells

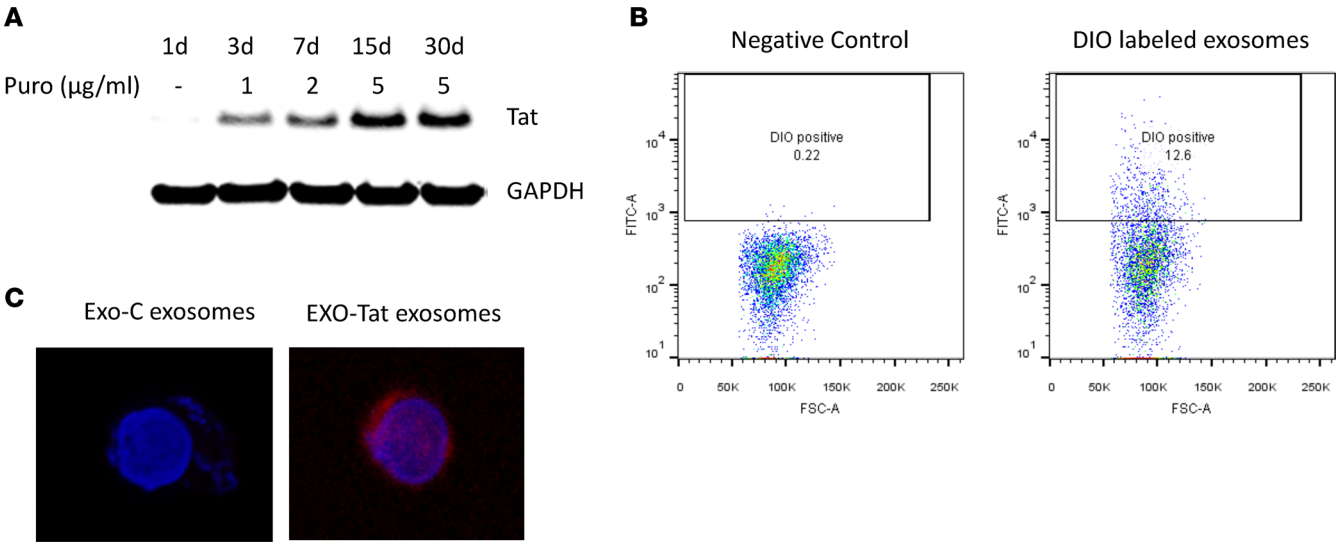


**Figure 4. Generation of exosomes loaded with Tat protein and their association with CD4⁺ T cells.** (**A**) A stable cell line expressing EXO-Tat was generated by transducing HEK293T cells with EXO-Tat lentiviruses and screened under the pressure of puromycin (Puro). After being cultured in 5 μg/ml Puro for 15 days, the cells expressed stable levels of Tat protein. (**B**) To quantify CD4⁺ T lymphocyte uptake, we isolated exosomes and labeled with the lipophilic dye DIO. Incubation of labeled exosomes with CD4⁺ T lymphocytes led to ~13% of cells acquiring dye, as quantified by flow cytometry. Unlabeled exosomes served as a control. (**C**) To visualize exosome association with CD4⁺ T lymphocytes, fluorescent dye–conjugated antibody was used, which recognizes EXO-Tat protein (Total magnification ×100). A representative CD4⁺ T lymphocyte with EXO-Tat exosomes is shown here. Exo-C exosomes, control exosomes.

from another 6 antiretroviral therapy–treated (ART-treated) individuals (patients #112, #204, #225, #108, #223, and #109 in Table 1), treated them with Exo-C and EXO-Tat exosomes or the global immune activator PMA/I for 4 days. The respective supernatants were subsequently cocultured with MOLT-4 cells, and viral p24 antigen in cell culture supernatants was quantified by ELISA. We found that EXO-Tat exosomes induced p24 production in 3 of 6 patient samples (Figure 5E).

*Exosomes can be engineered to target CD4⁺ cells, leading to improved latency reversal activity of EXO-Tat*. Limiting dilution assays reveal that ≤ 1 × $10^6$ rCD4⁺ T lymphocytes are infected with replication competent HIV-1 (7, 23, 24). We reasoned that exosomes made to specifically target CD4⁺-expressing cells would be more potent in terms of activating latent HIV-1. We modified exosomes by expressing EXO-Tat with a construct encoding an IL-16 C-terminal 20–amino acid domain fused to the N-terminus of lysosome-associated membrane protein 2 variant b (Lamp2b). Our rationale for using this approach derived from the fact that IL-16 is a natural ligand for the CD4 receptor, with the minimal peptide RRKS within the C-terminus of IL-16 being critical for CD4 receptor binding (25). The biologic activity of IL-16, however, resides in the N-terminus (26). To ensure exosomal membrane placement of this CD4⁺ receptor–targeting moiety, we fused the C-terminus of IL-16 with the extracellular domain of exosomal protein Lamp2b (27). We next generated a stable cell line producing CD4⁺ receptor–targeting exosomes harboring Tat ($EXO^{CD4}$-Tat). Compared with EXO-Tat, $EXO^{CD4}$-Tat led to a 20-fold increase in Tat protein delivery to CD4⁺ T lymphocytes, as quantified by Western blot of cellular lysates (Figure 6A). We next added an HA-tag to Tat in both EXO and $EXO^{CD4}$ preparations and used immunofluorescent imaging to visualize more efficient delivery of Tat to CD4⁺ cells (Figure 6B). To further confirm that $EXO^{CD4}$-Tat exosomes specifically target CD4⁺ cells, we purified CD4⁺ T cells and CD4⁻ cells from human peripheral blood mononuclear cells (PBMCs) obtained from health donors. Keeping total cell number constant, we varied the ratio between CD4⁺ and CD4⁻ cells (0%, 25%, 50%, or 100%) and treated cellular preparations with the same amount of $EXO^{CD4}$-Tat exosomes (100 μg) for 24 hours. Cell-associated Tat was quantified by Western blot. As shown in Figure 6C, Tat protein levels increased proportionally to the ratio of CD4⁺ T cells to CD4⁻ T cells. We next tested whether this increased CD4 targeting ability led to greater reactivation of latent HIV-1 in primary cells. We treated rCD4⁺ T cells from another 3 ART-treated patients (patients #230, #123, and #234 in Table 1) for 4 days and cocultured the supernatants with MOLT-4 cells, as previously described. $EXO^{CD4}$-Tat exosomes reactivated latent HIV-1 ex vivo in 3 of 3 individuals (Figure 6D).

**Table 1. Characteristics of study participants**

| Patient ID | Sex | Age | Race | CD4 | PVL | Year of Dx | <75 since | Medication |
|---|---|---|---|---|---|---|---|---|
| #211 | F | 51 | White | 884 | <20 | 1990 | 7/2012 | Stribild |
| #219 | F | 45 | White | 782 | <20 | 2009 | 6/2010 | Atripla |
| #232 | F | 58 | White | 945 | <20 | 1990 | 3/2009 | Atripla |
| #111 | M | 56 | White | 650 | <20 | 2001 | 4/2002 | Atripla |
| #207 | F | 55 | Black | 1392 | <20 | 2001 | 4/2003 | Ziagen, Reyataz |
| Norvir | | | | | | | | |
| #112 | M | 63 | Black | 853 | <20 | 1998 | 2/2001 | Truvada |
| Raltegravir | | | | | | | | |
| #204 | F | 44 | Black | 1503 | <20 | 1995 | 8/2012 | Stribild |
| #225 | F | 65 | White | 892 | <20 | 1991 | 3/2005 | Ziagen, Sustiva, 3TC |
| #108 | M | 55 | Black | 435 | <20 | 1990 | 12/2008 | Triumeq |
| #223 | F | 44 | White | 564 | <20 | 2005 | 2/2007 | Norvir, Truvada |
| Reyataz | | | | | | | | |
| #109 | M | 51 | White | 506 | <20 | 1986 | 7/2012 | Reyataz |
| #230 | F | 49 | White | 803 | <20 | 1988 | 8/2007 | Epzicom |
| Reyataz | | | | | | | | |
| #123 | M | 54 | White | 866 | <20 | 2005 | 12/2012 | Norvir, Epzicom, Prezista |
| #234 | F | 31 | White | 865 | <20 | 2002 | 3/2011 | Stribild |

F, female; M, male; PVL, plasma viral load. Dx, diagnosis. <75 since indicates a plasma viral load below 75 copies/ml of plasma.

*$EXO^{CD4}$-Tat exosomes have no significant effect on T cell activation, apoptosis, or cytokine release*. The potential toxicity of HIV-1 Tat is a concern when forwarding the protein as a therapeutic. In cell model and murine animal systems, Tat expression is associated with bystander cell death, apoptosis, and neuronal toxicity. We quantified the effect of $EXO^{CD4}$-Tat treatments (96 hours) on immune activation and apoptotic parameters of primary $rCD4^+$ T lymphocytes in culture. Neither control nor $EXO^{CD4}$-Tat exosomes altered the activation status of $rCD4^+$ T lymphocytes, as measured by FACS quantification of surface markers such as HLA-DR, CD-25, and CD-69 (Figure 7). Additionally, exosomal (control and $EXO^{CD4}$-Tat) treatment of $rCD4^+$ T cells had no significant effect on annexin V (Figure 7). Lastly, we also measured the expression levels of 12 proinflammatory cytokines and chemokines in the culture media of $rCD4^+$ T cells treated with control or $EXO^{CD4}$-Tat exosomes. As seen in Figure 8, exosomal treatment had no appreciable effect on the cytokine panel compared with treatments with PMA/I, which significantly increased the levels of IL-2, IL-17a, INF-γ, TNF-α, and GM-CSF.

## Discussion

HAART regimens suppress viral replication to levels below the detection limit of current assays and have significantly decreased the morbidity and mortality associated with HIV-1 infection (28). Despite this unbridled clinical success, a reservoir of replication competent HIV-1 persists even after prolonged treatment, thereby preventing viral cure (4). Current approaches to eradicate HIV-1 include pharmacologic approaches to reactivate latent virus with drugs such as histone deacetylase inhibitors (HDACi) and Dis (14, 29). While these agents reverse HIV-1 latency in vitro, clinical administration has not been associated with significant reductions in viral burden in vivo. The ability of the HIV-1 protein Tat to activate viral transcription has been long known, but few attempts have been made to harness the protein as an LRA. Potential toxicity and the practicality of generating sufficient amounts of clinical-grade protein product are major limitations. Here, we describe a potential strategy to overcome these limitations and lay the foundation for establishing exosomal preparations as a novel class of LRA.

Nanoparticles have been investigated as LRA delivery vehicles to reactivate latent HIV-1 (30). Exosomes can be thought of as endogenous nanoparticles generated by virtually every cell type examined. We used the HEK293T cell line as a factory for manufacturing exosomal Tat. Theoretically, every single exosome generated by the stable cells should contain Tat protein. Since the size of an exosome is that of a virus, it is technically hard, if not impossible, to determine the Tat expression in a single exosome. While Tat is released by HIV-1–infected cells (31, 32), the lack of appreciable secretion by the HEK293T cell line allowed us to

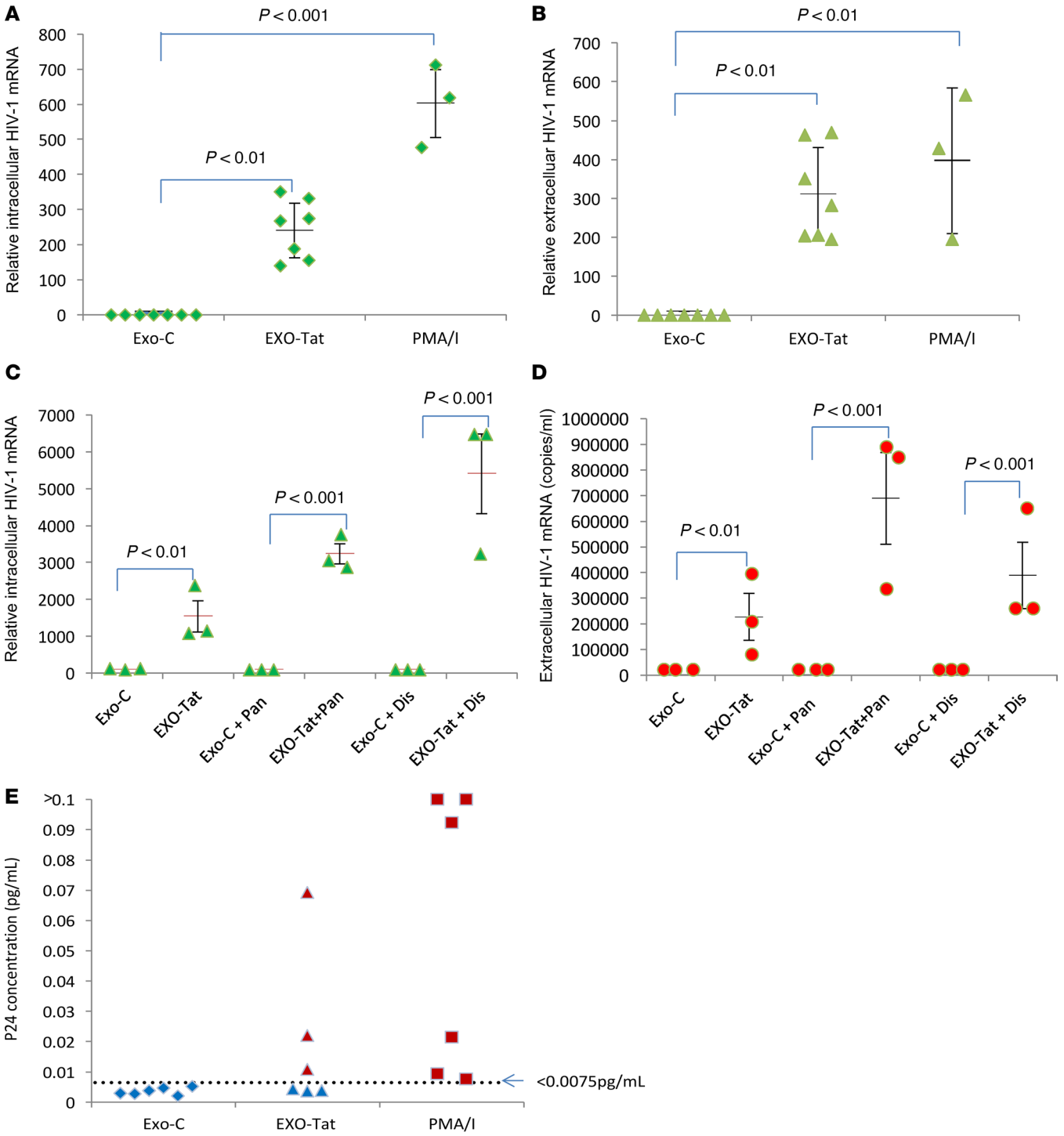


**Figure 5. EXO-Tat exosomes reactivate latent HIV-1 ex vivo in resting CD4⁺ (rCD4⁺) T cells.** rCD4⁺ T cells were isolated from the PBMCs of ART-treated patient blood. Two million rCD4⁺ T cells were treated with control exosomes (Exo-C), EXO-Tat exosomes (EXO-Tat), panobinostat (Pan), disulfiram (Dis), or PMA/I as indicated for 4 days. The cells and supernatants were separated by centrifugation. HIV-1 mRNA was determined by qPCR. P24 concentration in the supernatants was measured by ELISA. (**A**) EXO-Tat exosomes reactivated latent HIV-1 and increased its mRNA expression in cells. (**B**) EXO-Tat exosomes increased the release of HIV-1 mRNA into culture medium as detected by qPCR. (**C** and **D**) Comparison of the latency reversing potency of EXO-Tat exosomes with Pan or Dis. EXO-Tat exosomes synergistic effect with Pan or Dis, increasing HIV-1 mRNA expression in cells (**C**) or in supernatants (**D**). (**E**) EXO-Tat reactivated replication competent HIV-1 as measured by p24 concentration in the supernatants of 3/6 patient samples. The lowest limit of p24 quantification is 0.0075 pg/ml. Quantitative data was analyzed by ANOVA with between-group comparisons evaluated with post-hoc Tukey-Kramer HSD tests, which correct for multiple comparison. Data are expressed as mean ± SEM. $P < 0.05$ indicates statistical significance.

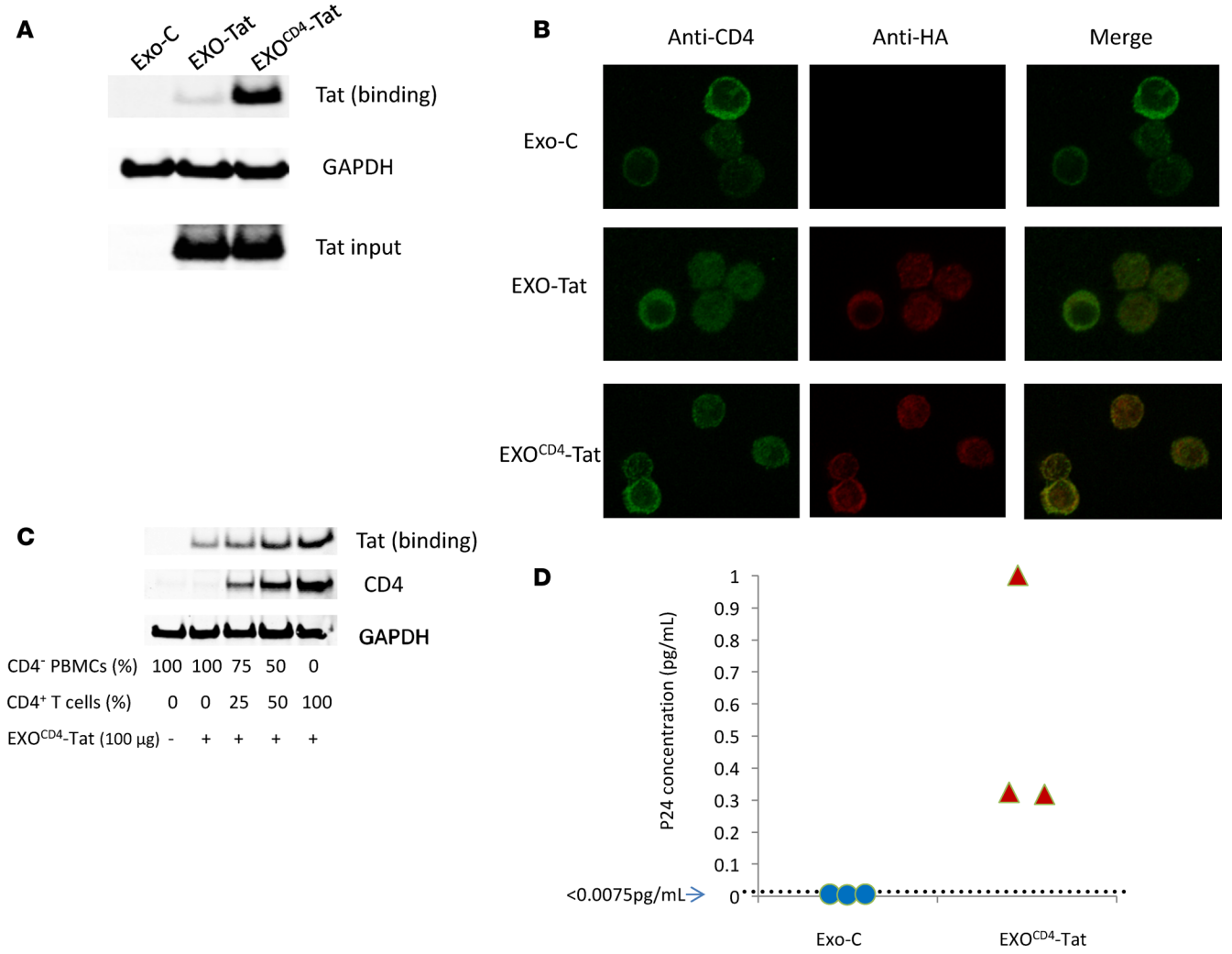


**Figure 6. EXO$^{CD4}$-Tat exosomes specifically target CD4$^+$ cells.** (**A**) Inclusion of a CD4$^+$ binding moiety in exosomes (EXO$^{CD4}$-Tat) increased CD4$^+$ T cell binding. Control Exosomes (Exo-C), EXO-Tat, or EXO$^{CD4}$-Tat exosomes were incubated with CD4$^+$ T cells for 24 hours, and Western blot was used to compare intracellular Tat levels in cells treated with EXO-Tat or EXO$^{CD4}$-Tat exosomes. GAPDH was used as a cell lysate loading control. Western blot band intensity was measured using the Licor Odyssey software. (**B**) EXO$^{CD4}$-Tat exosomes specifically target CD4$^+$ T cells. Exo-C, EXO-Tat, or EXO$^{CD4}$-Tat exosomes were incubated with PMBCs from healthy donors for 24 hours. The supernatants were removed by centrifugation. The cell pellets were prepared and probed with fluorescent conjugated antibodies, which recognize CD4 (green) or HA-tagged Tat (red). The top row shows CD4 staining (green). The middle row shows CD4 staining (green), Tat staining (red), and the merge of green and red. The bottom row shows CD4 staining (green), Tat staining (red), and the merge of green and red. The much stronger merged color orange indicates Tat protein containing exosomes binding to CD4$^+$ T cells. Total magnification × 100. (**C**) A representative data set of 2 independent Western blot results is shown here, indicating EXO$^{CD4}$-Tat exosomes specifically target CD4$^+$ cells. CD4$^-$ PBMCs were prepared by depleting CD4$^+$ cells from PBMCs using CD4 Dynabeads. CD4$^+$ T cells were isolated from PBMCs using Dynabeads Untouched Human CD4$^+$ T cells kit. CD4$^-$ PBMCs and CD4$^+$ T cells were mixed at the indicated ratio and incubated with or without the same amount of EXO$^{CD4}$-Tat exosomes (100 µg) for 24 hours. Cell-bound exosomes were measured by Western blot. (**D**) EXO$^{CD4}$-Tat exosomes reactivated latent HIV-1 from 3/3 patient samples, while control exosomes did not. The lowest limit of p24 quantification is 0.0075 pg/ml.

modify expression vectors to maximize exosomal Tat concentration. Here, we faced an initial experimental challenge in that exosomal localization compromised transactivating ability largely by sequestering Tat in nonnuclear compartments, as seen in our first generation of constructs. Although the addition of a c-Myc NLS increased transactivation activity as quantified by in vitro models of viral latency, the efficacy in primary rCD4$^+$ T lymphocytes was poor, with viral reactivation leading to replication-competent virion progeny in 3 of 6 cases. This prompted us to address perhaps the biggest challenge in exosomal therapeutics — namely, targeting exosomes to specific cellular populations. Our experiments revealed that HEK293T-produced exosomes were able to discharge cargo into ~13% of purified CD4$^+$ T lymphocytes following coculture for 24 hours. Current data suggest that latent HIV-1 burden is surprisingly low after multiyear effective antiretroviral therapy, with perhaps 1 in 1 million rCD4$^+$ T lymphocytes harboring replication-competent HIV-1 (3, 7,

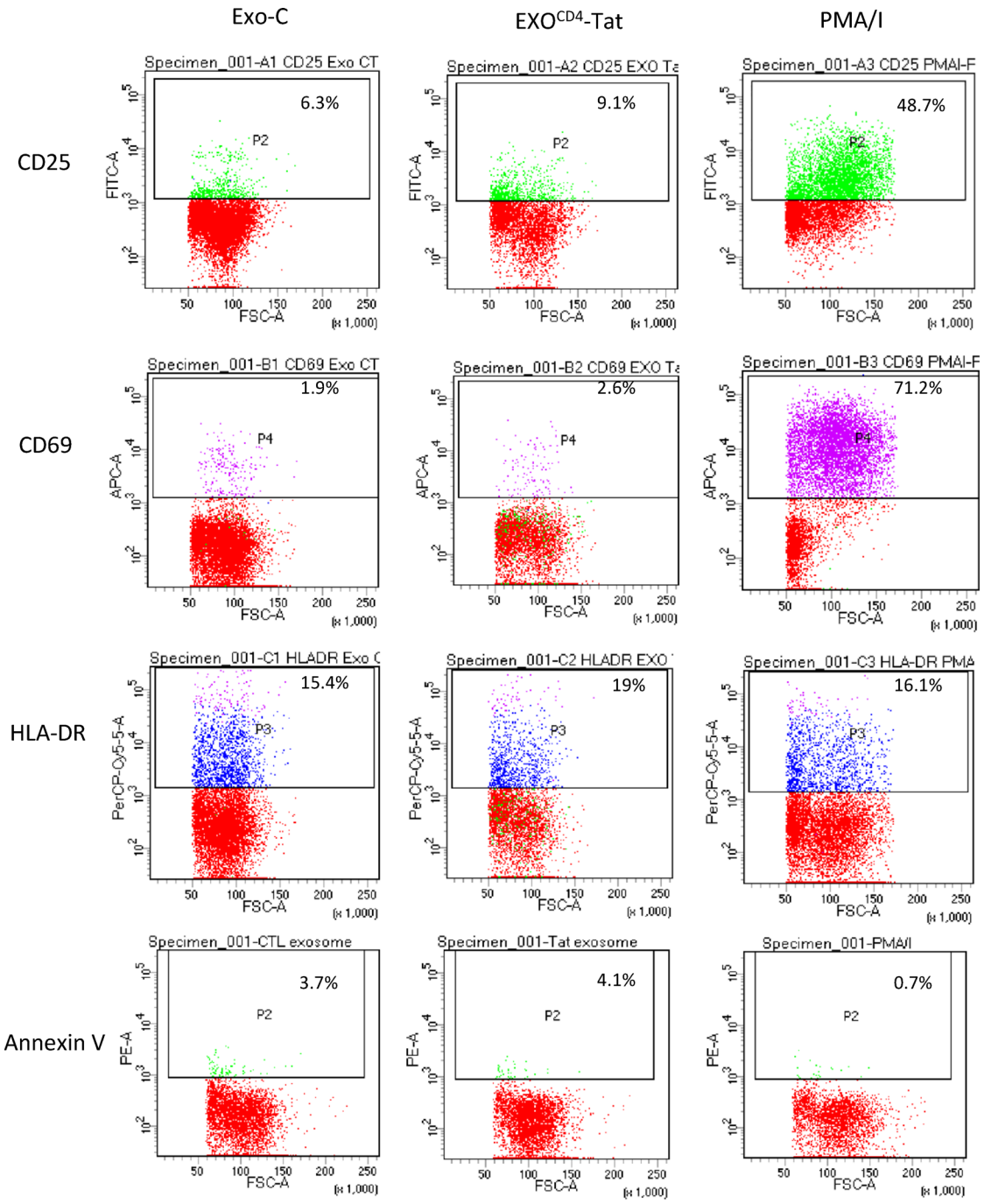


**Figure 7. Effect of EXO$^{CD4}$-Tat exosomes on T cell activation.** Resting CD4$^+$ T cells were isolated from PBMCs of healthy donors and treated with control exosomes (Exo-C), EXO$^{CD4}$-Tat exosomes, or PMA/I for 2 days. The cells and supernatants were separated by centrifugation. A representative data set of 3 independent experiments showing the expression levels of T cell activation markers CD25, CD69, and HLA-DR measured by flow cytometry. EXO$^{CD4}$-Tat exosomes had no significant impact on those markers.

13, 24). Clearly, LRAs based on an exosomal delivery platform will need precision targeting with the ability to deliver cargo specifically to rCD4$^+$ T lymphocytes. To this end, we recapitulated the natural ligand/receptor interaction between the IL-16/CD4$^+$ receptor by expressing the C-terminal motifs of IL-16 responsible for CD4$^+$ receptor binding in conjunction with the exosomal membrane protein Lamp2b. These molecular manipulations increased rCD4$^+$ T lymphocyte uptake of exosomes by 20-fold, with attendant increase in latency reversal potency. Exosomal targeting of rCD4$^+$ T lymphocytes led to viral reactivation and production of replication-competent HIV-1 in 3 of 3 individuals tested.

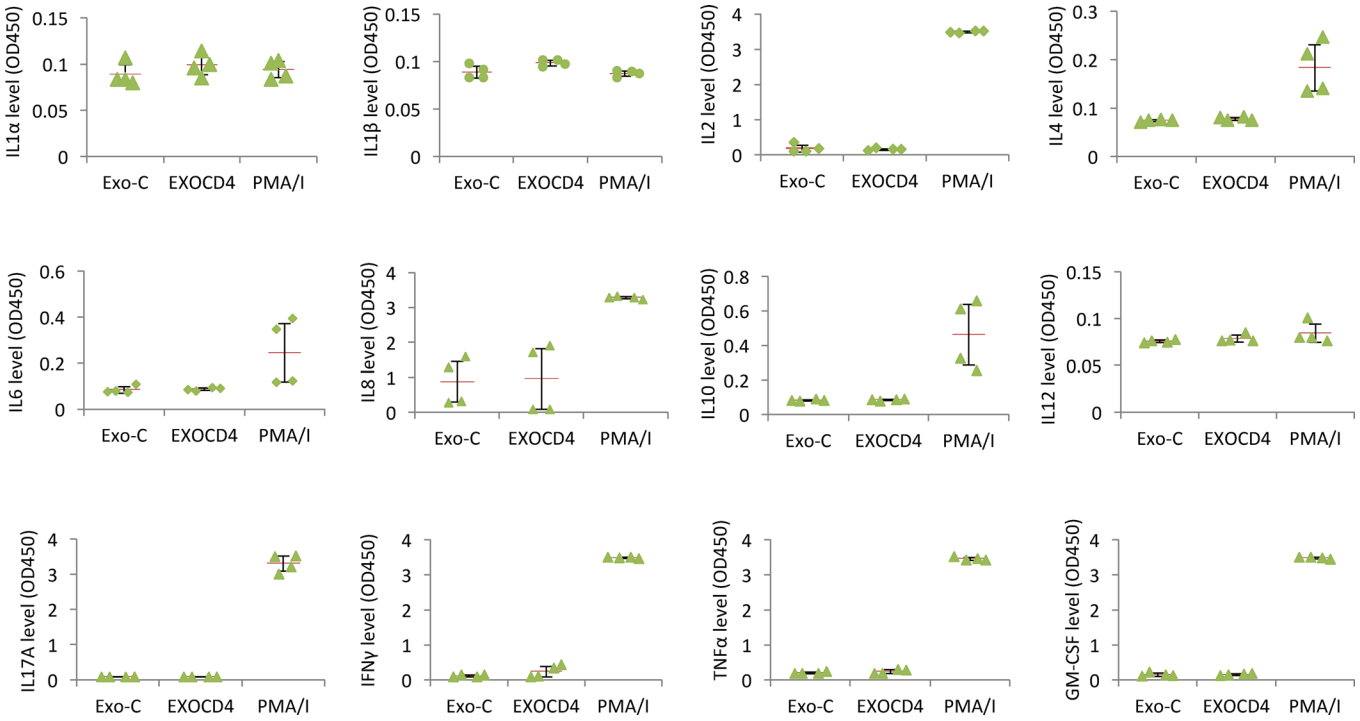


**Figure 8. Effect of EXO$^{CD4}$-Tat exosomes on cytokine release.** Resting CD4$^+$ T cells were isolated from PBMCs of healthy donors and treated with control exosomes (Exo-C), EXO$^{CD4}$-Tat exosomes, or PMA/I for 2 days. The cells and supernatants were separated by centrifugation. The expression levels of proinflammatory cytokines (IL-1α, IL-1β, IL-2, IL-4, IL-6, IL-8, IL-10, IL-12, IL-17a, IFN-γ, TNF-α, and GM-CSF) in the supernatants were measured using a Multi-Analyte ELISArray Kit. EXO$^{CD4}$-Tat exosomes had no significant effect on the release of proinflammatory cytokines. PMA/I substantially increased the release of IL-2, IL-4, IL-6, IL-8, IL-10, IL-17a, IFN-γ, TNF-α, and GM-CSF. EXOCD4, EXO$^{CD4}$-Tat exosomes.

As mentioned, a potential challenge in forwarding Tat-based therapeutics is toxicity. Our experiments did not find that exosomal Tat impacted cellular activation, levels of apoptosis, or inflammatory cytokine release. These experiments were conducted using in vitro experimentation on primary rCD4$^+$ T lymphocytes to determine whether the latency reversal we observed was a byproduct of generalized immune stimulation or specific HIV-LTR activation. Our results suggest the latter as a mechanism of action. Work by other groups has documented the relative safety of Tat protein administration in animal models and humans (16, 32, 33). For example, 2 recent human trials have used WT Tat protein as an immunogen and found that up to 30 μg Tat intradermal injections were well tolerated with no serious adverse events related specifically to Tat-mediated cytotoxicity (33, 34). Further work needs to be done to better characterize exosomal Tat from a pharmacologic toxicity point of view.

HIV-1 Tat is critical for the efficient replication of virus. Our work suggests that it may be possible to use this component of the virus itself as a means of purging the latent reservoir of infected cells. It is unlikely that Tat can target all latent virus and probably favors those proviruses in which transcription has been initiated. Future studies must focus on sequencing viral strains that emerge after exosomal Tat treatment and compare them with those that emerge after conventional LRA treatment to better quantify the totality of latency activation. Similarly, even if latent virus is reactivated, it is unclear whether this will lead to immune clearance of cells without additional therapeutic maneuvers such as administration of dual-affinity retargeting (DART) molecules (35, 36). Clinical translation of our approach will require validation in relevant preclinical models. While exosomes have been administered to experimental animals after in vitro generation, such an approach is tedious and certainly not practical in human trials (37). Our work demonstrates that lentiviral vectors can be efficiently used to deliver the construct encoding exosomal Tat. Similar approaches could be pursued with other viral vectors currently used in HIV-1 vaccine approaches, such as adeno-associated virus (AAV). Serial administrations of viral vectors encoding EXO-Tat in the setting of virological suppression, stable antiretroviral therapy, and conventional LRA treatment may serve as a foundation for a test-treat-transactivate paradigm for HIV-1 eradication.

## Methods

*Cell culture and transfection*. HEK293T cells were cultured in DMEM (Invitrogen) with 10% FBS (Thermo Fisher Scientific), 2 mM L-glutamine, and nonessential amino acids (Invitrogen). U1 cells, primary human PBMCs, and $CD4^+$ T cells were cultured in RPMI Medium 1640 (Invitrogen) with 10% FBS. TZM-bl cells were cultured in DMEM with 10% FBS, 4 mM L-glutamine, and nonessential amino acids. J-Lat GFP (clone A72) cells were cultured in RPMI Medium 1640 (Life Technologies) with 10% FBS, supplemented with 2 mM l-glutamine, penicillin G (100 U/ml) and streptomycin (100 μg/ml) (Life Technologies). Adherent cells were trypsinized and reseeded in culture plates 1 day before transfection or chemical treatment. HEK293T cells were transfected with Lipofectamine (Thermo Fisher Scientific) when cell confluency was ~70%. TZM-bl cells were transfected with Lipofectamine 2000, GenJet Plus DNA Transfection Reagent (SignaGen Laboratories), or Lipofectamine LTX Plus Reagent (Invitrogen). For generation of exosomes and testing their function, regular FBS was replaced by exosome-depleted FBS (System Biosciences) in the culture media of HEK293T, U1, and TZM-bl cells.

*Molecular cloning*. Using XPack Exosome Protein Engineering Technology (System Biosciences), the cDNA fragment encoding HIV-1 Tat protein with c-Myc NLS fused to its C-terminus was subcloned into XPack CMV-XP-MCS-EF1-Puro Cloning Lentivector between enzyme sites BamHI and EcoRI. The original HIV-1 Tat plasmid was ordered from Addgene (plasmid 14654) (38). The generated construct was named EXO-Tat. The cDNA fragment encoding the C-terminal domain of IL-16 fused to the N-terminus of Lamp2b was cloned into pCDH-EF1-MCS-T2A-Puro (System Biosciences) Cloning Lentivector between enzyme sites SwaI and NotI. The generated construct was named pIL-16lamp2b. For the sequences of primers used for molecular cloning, please see supplementary Supplemental Table 1 (supplemental material available online with this article; https://doi.org/10.1172/jci.insight.95676DS1). All constructs were sequenced at Yale Keck Biotechnology Resource Laboratory.

*Generation of lentivirus*. A lentiviral packaging plasmid pPACKH1 (System Biosciences) was cotransfected into HEK293T cells with an empty vector (EV; XPack CMV-XP-MCS-EF1-Puro Cloning Lentivector), pEXO-Tat, pIL16lamp2b, or pIL16lam2b plus pEXO-Tat at the ratio 2:1 to generate control lentiviruses, EXO-Tat lentiviruses, IL16lamp2b lentiviruses, or $EXO^{CD4}$-Tat lentiviruses, respectively. The supernatants of the transfected cells were collected at 48 and 96 hours after transfection. The combined supernatants were filtered through a 0.45-μm Millex-HV Filter Unit (MilliporeSigma). Lentiviruses were concentrated with PEG-it Virus Precipitation Solution (System Biosciences). The titers of viruses were determined with the UltraRapid Lentiviral Titer Kit (System Biosciences) following the manufacturer's instructions.

*Generation of stable cell lines*. Four lines of cells stably expressing an EV (XPack CMV-XP-MCS-EF1-Puro Cloning Lentivector), pEXO-Tat, IL16lamp2b, or pEXO-Tat plus pIL16lamp2b were generated by transducing HEK293T cells with the above mentioned lentiviruses at a multiplicity of infection (MOI) of 10. Three days after transfection, puromycin (1 μg/ml) was added to the culture medium to eliminate untransfected cells. To select cells with high Tat gene incorporation, puromycin concentration was increased to 5 μg/ml. The supernatants of stable cells were collected for isolation of exosomes. Tat protein expression was confirmed by Western blot.

*Exosome isolation and characterization*. Stable cells were cultured in media with exosome-depleted FBS. Supernatants of the stable cells were collected and used for isolation of exosomes using differential ultracentrifugation method: 300 *g* for 10 minutes; 2,000 *g* for 30 minutes; 10,000 *g* for 30 minutes; and 100,000 *g* for 60 minutes. The last pellets were exosomes (37). Exosomes were washed once with plain RPMI medium. The exosomes were suspended in plain RPMI medium and stored either at 4°C for 1–7 days or at –80°C for further use. The number and size distribution of exosomes were determined on a NanoSight NS500 (Malvern Instruments) with a syringe pump.

*Exosome labeling and uptake*. Exosomes were directly labeled with 1 μM Vybrant Cell Tracers DIO (Invitrogen) by incubation for 30 minutes at 37°C and then washed twice by ultracentrifugation at 100, 000 *g* for 1 hour in 1× PBS (37). Labeled exosomes were cocultured with $CD4^+$ T cells for 24 hours and washed with PBS twice. Cells were analyzed on a BD Bioscience LSRII with FACS Diva 8.0.1. DIO fluorescence was excited from a 488 nm laser and detected through a 505 LP and 530/30 nm filter. Cells were separated from debris by utilizing a forward vs. side scatter dot plot. Twenty thousand events were collected for each sample. Analysis and figure preparation was performed using FlowJo v10 software.

*Primary antibodies and primers*. HA (6E2; catalog 2367), GFP (4B10; catalog 2955), and Alix (3A9; catalog 2171) mouse monoclonal antibodies were purchased from Cell Signaling Technology. GAPDH

(0411; catalog sc-47724) mouse monoclonal antibody and GAPDH (FL-335; catalog sc-25778) rabbit polyclonal antibody were purchased from Santa Cruz Biotechnology Inc. Lamp2b (catalog ab18529) rabbit polyclonal antibody was from Abcam. Alexa Fluor 594 HA-tag mAb (16B12; catalog A-21288), human CD4 Alexa Fluor 488 mAb (S3.5; catalog MHCD0420), and human CD8 Alexa Fluor 647 mAb (3B5; catalog MHCD0821) were from Thermo Fisher Scientific. All primers were ordered from Integrated DNA Technologies and listed in Supplemental Table 1.

*Subcellular fractionation*. Subcellular fractionation was performed using Subcellular Protein Fractionation Kit for Cultured Cells (Thermo Fisher Scientific) according to the manufacturer's instructions. Briefly, cells were harvested and washed once with cold PBS. Cells were then suspended in CEB buffer and rotated at 4°C for 10 minutes. After centrifugation at 500 *g* at 4°C for 5 minutes, supernatant was collected as the cytoplasmic fraction. The pellets were suspended in membrane extraction buffer and rotated at 4°C for 10 minutes. After centrifugation at 3,000 *g* at 4°C for 5 minutes, supernatant was collected as the membranous fraction. The pellets were washed in MEM buffer twice and finally lysed in Pierce IP lysis buffer (Thermo Fisher Scientific) as the nuclear fraction.

*Western blot*. Protein samples were prepared in Pierce IP lysis buffer (Thermo Fisher Scientific). Protein (10–20 μg) was mixed with NuPAGE LDS Samples Buffer (Invitrogen) and separated by 4-12% NuPAGE Novex 4-12% Bis-Tris gel electrophoresis and electroblotted to nitrocellulose membrane (Bio-Rad). Blotted membranes were probed with their respective primary antibodies, rotating at 4°C overnight. Membranes were washed 3 times in TBST buffer and probed with secondary antibody (680 goat anti–rabbit IgG or IRDye800-conjugated affinity purified anti–mouse IgG, respectively) at room temperature for 1 hour. Membranes were then washed 3 times in TBST buffer, and direct infrared fluorescence detection was performed with a Licor Odyssey Infrared Imaging System (39).

*Luciferase assay*. EV, pTat, pXO-Tat, or pEXO-Tat was transfected into TZM-bl cells when the cells were at about 60%–70% confluence. Forty-eight hours after transfection, luciferase activity was performed using the Dual-Glo Luciferase Assay System (Promega). For each experiment, a control employing an EV was used, and corrected luciferase values were averaged, arbitrarily set to a value of "1", and served as a reference for comparison of fold differences in experimental values (40).

*HIV-1 p24 ELISA assay*. Exosomes were added to U1 culture medium containing exosome-depleted FBS. Forty-eight hours after addition of exosomes, U1 cell culture media were collected and used for p24 ELISA assay using a p24 ELISA Kit (PerkinElmer) according the manufacturer's instructions. The analytical sensitivity of the kit is 17.1 pg/ml.

*Study subjects*. HIV-1–infected individuals were enrolled in the study at The Miriam Hospital based on the criteria of suppressive ART and undetectable plasma HIV-1 RNA levels (<50 copies per ml) for a minimum of 12 months. Characteristics of study participants are presented in Table 1.

*Isolation and culture of resting CD4$^+$ T cells*. PBMCs from whole blood or buffy coats of healthy donors were purified using density centrifugation on a Ficoll-Hypaque (GE Healthcare) gradient. Resting CD4$^+$ T cells (CD4$^+$, CD25$^-$, CD69$^-$, and HLA-DR$^-$) were isolated by negative depletion using sequential combination of a human CD4$^+$ T cell isolation kit, human CD25 MicroBeads II, a human CD69 MicroBead Kit II, and a human anti–HLA-DR MicroBeads kit (Miltenyi Biotec) (7, 24). Cells were cultured in RPMI medium with 10% FBS at a concentration of $2 \times 10^6$ cells per 0.6 ml for all experiments. For treatment, 50 μl of exosomes ($1.8 \times 10^9$ exosomes or 46.8 μg total protein) or 50 ng/ml PMA plus 1 μM ionomycin was added to 450 μl culture medium of rCD4$^+$ T cells.

*Measurement of intracellular and extracellular HIV-1 mRNA*. Two million rCD4$^+$ T cells were treated with EXO-C, Tat exosomes (EXO-Tat), or PMA/I for 4 days. The cells and supernatants were separated by centrifugation. Total RNA from the cells was used to detect intracellular HIV-1 mRNA; total RNA from supernatants was used to detect extracellular HIV-1 mRNA following the method established by Silicano laboratory (see ref. 7).

*Flow cytometry*. rCD4$^+$ T cells were treated with Exo-C, engineered exosomes, or PMA/I for 48 hours. The cells were subsequently used for measurement of T cell activation markers (CD25, CD69, and HLA-DR) or apoptosis marker annexin V. For detecting T cell activation, FITC mouse anti–human CD25 (BD Pharmingen), APC mouse anti–human CD69 (BD Pharmingen), and PerCP-Cy 5.5 mouse anti–human HLA-DR (BD Pharmingen) were used to stain the cells. For early apoptosis detection, PE Annexin V (BD Pharmingen) was used to stain the cells. Cells were analyzed on a BD Bioscience LSRII with FACS Diva 8.0.1. Analysis and figure preparation was performed using FlowJo V10 software.

*HIV-1 p24 antigen assay*. The Simoa p24 antigen assay is a 2-step digital immunoassay to measure the quantity of p24 using the Simoa HD-1 Analyzer and Single Molecule Array (Simoa) technology with an analytical sensitivity of 0.0074 pg/ml. Resting $CD4^+$ T cells were isolated from the PBMCs of the blood of HIV-1 patients who were treated with ART for a period of time. Resting $CD4^+$ T cells were treated with exosomes or PMA/I for 4 days. The supernatants were collected and cocultured with MOLT-4 cells to amplify HIV-1 virus. The supernatants from treated resting $CD4^+$ T cells or from cocultured MOLT-4 cells were used to measure p24 concentration.

*Immunocytochemistry*. For viewing the random interaction between exosomes and cells, $CD4^+$ T cells were isolated from the PBMCs of a healthy donor using a Dynabeads Untouched Human CD4 T cells isolation kit (Invitrogen) and cultured in RPMI medium with 10% exosome-depleted FBS. The cells were treated with control (EV) or Exo-Tat exosomes for 24 hours. The cells were separated from culture medium by centrifugation and washed with PBS. The cells were fixed in 4% paraformaldehyde for 10 minutes and washed 3 times in PBS. Subsequently, cells were spread on Polysine Microscope Slides (Thermo Fisher Scientific) and blocked in normal mouse serum (Thermo Fisher Scientific) for 1 hour. Cells were stained with HA mAb overnight and washed 3 times in PBS. Cells were incubated with Alexa Fluor 594 goat anti–mouse IgG (Invitrogen) for 1 hour and washed 3 more times before taking immunofluorescent images. For testing exosomes specifically targeting $CD4^+$ cells, PBMCs from healthy donors were treated with Exo-C, EXO-Tat exosomes, or $EXO^{CD4}$-Tat exosomes for 24 hours. The immunocytochemical procedure was similar, but the fluorescence-labeled primary antibodies were utilized.

*Immunofluorescent imaging*. Confocal images were acquired with a Nikon C1si confocal (Nikon Inc.) using diode lasers 402, 488, 561, and 638. Serial optical sections were performed with EZ-C1 computer software (Nikon Inc.). Each wavelength was acquired separately by invoking frame lambda. Z series sections were collected at 0.15 μm with a 100× Plan Apo lens and scan zoom of 2. Deconvolution and projections were performed in Elements version 3.2 (Nikon Inc.) computer software.

*Cytokine release assay*. $rCD4^+$ T cells were isolated from PBMCs of healthy donors and incubated with Exo-C, EXO-Tat/IL-16 lamp2b exosomes or PMA/I for 4 days. Culture supernatants were collected by centrifugation and used for cytokine assay. The concentration of 12 proinflammatory cytokines and chemokines (IL-1α, IL-1β, IL-2, IL-4, IL-6, IL-8, IL-10, IL-12, IL-17A, IFN-γ, TNF-α, and GM-CSF) in the supernatants were measured using a Multi-Analyte ELISArray Kit (Qiagen) following the manufacturer's instructions.

*Statistics*. Quantitative data of three or more groups was analyzed by two-way ANOVA with between-group comparisons evaluated with post-hoc Tukey-Kramer HSD tests, which correct for multiple comparison. Comparisons between two groups were carried out using Student's *t* test function with 2-tailed distribution. Data are expressed as mean ± SEM. $P < 0.05$ indicates statistical significance.

*Study approval*. The study was approved by Lifespan IRB. All research participants enrolled in the study provided written, informed consent prior to inclusion in this study. The approval numbers are FWA-Rhode Island Hospital (RIH) 00001230 and The Miriam Hospital (TMH) 00003538.

## Author contributions

XT and BR designed the experiments. XT and HL performed the experiments. MD performed the FACS measurements. SC performed phlebotomy and isolation of PBMCs from ART-treated patients. XT, PJQ, and BR coordinated the research. XT and BR wrote the manuscript. All authors discussed and interpreted the data and revised the manuscript.

## Acknowledgments

We thank the study participants, without whom this research would not be possible. We also thank Sicheng Wen and Yan Cheng for technical support in preparation of exosomes and Ginny Hovanesian for assistance in fluorescent imaging. This study was supported by NIH (R01HD072693, P30GM110759, K24HD080539 to BR) and Lifespan/Brown/Tufts CFAR (P30AI042853), P01AA019072, U54GM115677 and P20GM119943. The following reagent was obtained through the NIH AIDS Reagent Program, Division of AIDS, NIAID, NIH: TZM-bl from John C. Kappes, Xiaoyun Wu, and Tranzyme Inc. J-Lat GFP cells (clone A72) were from Eric Verdin and HIV-1–infected U937 cells (U1) were from Thomas Folks.

Address correspondence to: Bharat Ramratnam, Laboratory of Retrovirology, 55 Claverick Street (Laboratory 414), Providence, Rhode Island 02903, USA. Phone: 401.444.5219; Email: BRamratnam@Lifespan.org.

1. Chun TW, Moir S, Fauci AS. HIV reservoirs as obstacles and opportunities for an HIV cure. *Nat Immunol*. 2015;16(6):584–589.
2. Ruelas DS, Greene WC. An integrated overview of HIV-1 latency. *Cell*. 2013;155(3):519–529.
3. Siliciano JD, Siliciano RF. HIV-1 eradication strategies: design and assessment. *Curr Opin HIV AIDS*. 2013;8(4):318–325.
4. Dahabieh MS, Battivelli E, Verdin E. Understanding HIV latency: the road to an HIV cure. *Annu Rev Med*. 2015;66:407–421.
5. Archin NM, Sung JM, Garrido C, Soriano-Sarabia N, Margolis DM. Eradicating HIV-1 infection: seeking to clear a persistent pathogen. *Nat Rev Microbiol*. 2014;12(11):750–764.
6. Sgarbanti M, Battistini A. Therapeutics for HIV-1 reactivation from latency. *Curr Opin Virol*. 2013;3(4):394–401.
7. Laird GM, et al. Ex vivo analysis identifies effective HIV-1 latency-reversing drug combinations. *J Clin Invest*. 2015;125(5):1901–1912.
8. Zhang L, et al. Quantifying residual HIV-1 replication in patients receiving combination antiretroviral therapy. *N Engl J Med*. 1999;340(21):1605–1613.
9. Rasmussen TA, Tolstrup M, Søgaard OS. Reversal of Latency as Part of a Cure for HIV-1. *Trends Microbiol*. 2016;24(2):90–97.
10. Katlama C, et al. Barriers to a cure for HIV: new ways to target and eradicate HIV-1 reservoirs. *Lancet*. 2013;381(9883):2109–2117.
11. Sgro C. Side-effects of a monoclonal antibody, muromonab CD3/orthoclone OKT3: bibliographic review. *Toxicology*. 1995;105(1):23–29.
12. Ke R, Lewin SR, Elliott JH, Perelson AS. Modeling the Effects of Vorinostat In Vivo Reveals both Transient and Delayed HIV Transcriptional Activation and Minimal Killing of Latently Infected Cells. *PLoS Pathog*. 2015;11(10):e1005237.
13. Xing S, Siliciano RF. Targeting HIV latency: pharmacologic strategies toward eradication. *Drug Discov Today*. 2013;18(11-12):541–551.
14. Rasmussen TA, et al. Panobinostat, a histone deacetylase inhibitor, for latent-virus reactivation in HIV-infected patients on suppressive antiretroviral therapy: a phase 1/2, single group, clinical trial. *Lancet HIV*. 2014;1(1):e13–e21.
15. Razooky BS, Pai A, Aull K, Rouzine IM, Weinberger LS. A hardwired HIV latency program. *Cell*. 2015;160(5):990–1001.
16. Lin X, et al. Transcriptional profiles of latent human immunodeficiency virus in infected individuals: effects of Tat on the host and reservoir. *J Virol*. 2003;77(15):8227–8236.
17. Geng G, et al. Development of an Attenuated Tat Protein as a Highly-effective Agent to Specifically Activate HIV-1 Latency. *Mol Ther*. 2016;24(9):1528–1537.
18. de Gassart A, Geminard C, Fevrier B, Raposo G, Vidal M. Lipid raft-associated protein sorting in exosomes. *Blood*. 2003;102(13):4336–4344.
19. Derdeyn CA, et al. Sensitivity of human immunodeficiency virus type 1 to the fusion inhibitor T-20 is modulated by coreceptor specificity defined by the V3 loop of gp120. *J Virol*. 2000;74(18):8358–8367.
20. Folks TM, Justement J, Kinter A, Dinarello CA, Fauci AS. Cytokine-induced expression of HIV-1 in a chronically infected promonocyte cell line. *Science*. 1987;238(4828):800–802.
21. Jordan A, Bisgrove D, Verdin E. HIV reproducibly establishes a latent infection after acute infection of T cells in vitro. *EMBO J*. 2003;22(8):1868–1877.
22. Procopio FA, et al. A Novel Assay to Measure the Magnitude of the Inducible Viral Reservoir in HIV-infected Individuals. *EBioMedicine*. 2015;2(8):874–883.
23. Laird GM, Rosenbloom DI, Lai J, Siliciano RF, Siliciano JD. Measuring the Frequency of Latent HIV-1 in Resting $CD4^+$ T Cells Using a Limiting Dilution Coculture Assay. *Methods Mol Biol*. 2016;1354:239–253.
24. Bullen CK, Laird GM, Durand CM, Siliciano JD, Siliciano RF. New ex vivo approaches distinguish effective and ineffective single agents for reversing HIV-1 latency in vivo. *Nat Med*. 2014;20(4):425–429.
25. Keane J, et al. Conservation of structure and function between human and murine IL-16. *J Immunol*. 1998;160(12):5945–5954.
26. Nicoll J, Cruikshank WW, Brazer W, Liu Y, Center DM, Kornfeld H. Identification of domains in IL-16 critical for biological activity. *J Immunol*. 1999;163(4):1827–1832.
27. Alvarez-Erviti L, Seow Y, Yin H, Betts C, Lakhal S, Wood MJ. Delivery of siRNA to the mouse brain by systemic injection of targeted exosomes. *Nat Biotechnol*. 2011;29(4):341–345.
28. Simon V, Ho DD, Abdool Karim Q. HIV/AIDS epidemiology, pathogenesis, prevention, and treatment. *Lancet*. 2006;368(9534):489–504.
29. Xing S, et al. Disulfiram reactivates latent HIV-1 in a Bcl-2-transduced primary CD4+ T cell model without inducing global T cell activation. *J Virol*. 2011;85(12):6060–6064.
30. Kovochich M, Marsden MD, Zack JA. Activation of latent HIV using drug-loaded nanoparticles. *PLoS One*. 2011;6(4):e18270.
31. Ensoli B, et al. Release, uptake, and effects of extracellular human immunodeficiency virus type 1 Tat protein on cell growth and viral transactivation. *J Virol*. 1993;67(1):277–287.
32. Chang HC, Samaniego F, Nair BC, Buonaguro L, Ensoli B. HIV-1 Tat protein exits from cells via a leaderless secretory pathway and binds to extracellular matrix-associated heparan sulfate proteoglycans through its basic region. *AIDS*. 1997;11(12):1421–1431.
33. Ensoli F, et al. HIV-1 Tat immunization restores immune homeostasis and attacks the HAART-resistant blood HIV DNA: results of a randomized phase II exploratory clinical trial. *Retrovirology*. 2015;12:33.
34. Ensoli B, et al. The preventive phase I trial with the HIV-1 Tat-based vaccine. *Vaccine*. 2009;28(2):371–378.
35. Sung JA, et al. Dual-Affinity Re-Targeting proteins direct T cell-mediated cytolysis of latently HIV-infected cells. *J Clin Invest*. 2015;125(11):4077–4090.
36. Sloan DD, et al. Targeting HIV Reservoir in Infected CD4 T Cells by Dual-Affinity Re-targeting Molecules (DARTs) that Bind HIV Envelope and Recruit Cytotoxic T Cells. *PLoS Pathog*. 2015;11(11):e1005233.
37. Wen S, et al. Mesenchymal stromal cell-derived extracellular vesicles rescue radiation damage to murine marrow hematopoietic cells. *Leukemia*. 2016;30(11):2221–2231.
38. Cujec TP, et al. The HIV transactivator TAT binds to the CDK-activating kinase and activates the phosphorylation of the carboxy-terminal domain of RNA polymerase II. *Genes Dev*. 1997;11(20):2645–2657.
39. Tang X, et al. Acetylation-dependent signal transduction for type I interferon receptor. *Cell*. 2007;131(1):93–105.
40. Tang X, Zhang Y, Tucker L, Ramratnam B. Phosphorylation of the RNase III enzyme Drosha at Serine300 or Serine302 is required for its nuclear localization. *Nucleic Acids Res*. 2010;38(19):6610–6619.